Strong interband interaction in the excitonic insulator phase of Ta$_2$NiSe$_5$

Jinwon Lee,[1,2] Chang-Jong Kang,[3] Man Jin Eom,[2] Jun Sung Kim,[1,2] Byung Il Min,[2] and Han Woong Yeom[1,2,*]

[1]*Center for Artificial Low Dimensional Electronic Systems, Institute for Basic Science (IBS), Pohang 37673, Republic of Korea*
[2]*Department of Physics, Pohang University of Science and Technology, Pohang 37673, Republic of Korea*
[3]*Department of Physics and Astronomy, Rutgers University, Piscataway, New Jersey 08854, USA*

Excitonic insulator (EI) was proposed in the 1960s as a distinct insulating state originating from pure electronic interaction, but its material realization has been elusive with extremely few material candidates and with only limited evidence such as anomalies in transport properties, band dispersions, or optical transitions. We investigate the real-space electronic states of the low-temperature phase in Ta$_2$NiSe$_5$ with atomic resolution to clearly identify the quasiparticle energy gap together with the strong electron-hole band renormalization using scanning tunneling microscopy and spectroscopy (STS). These results are in good agreement with the EI transition scenario in Ta$_2$NiSe$_5$. Our spatially resolved STS data and theoretical calculations reveal further the orbital inversion at band edges, which indicates the exciton condensation close to the Bardeen-Cooper-Schrieffer regime.

Many-body interactions in metallic solids often induce insulating states such as Mott insulators through electron-electron interactions and Peierls insulators through electron-phonon interactions [1]. Excitonic insulator (EI) is another type of interaction-driven insulators formed through a purely electronic mechanism from semimetals or semiconductors with small energy gaps [2,3]. A valence electron excited to a conduction band leaves a hole in the valence band, and they can pair into an exciton [4]. When the carrier concentration and the dielectric constant are unusually small, the hole potential is poorly screened leading to enhanced exciton binding energy greater than the energy gap of the system. Then, the spontaneous exciton formation occurs and these bosonic quasiparticles condense into the same ground state. This unusual condensate, called the EI, results in flat band edges and an enlarged energy gap [2]. In a semimetal, the electron-hole interaction is relatively weak and the phase transition follows the same way as the condensation of Cooper pairs in Bardeen-Cooper-Schrieffer (BCS) superconductors, while the attractive interaction is strong in a semiconductor and the transition corresponds to the Bose-Einstein condensation of excitons [5].

While the EI idea was conceived as early as 1967 and demonstrated in artificial double layer systems with gate voltages or strong magnetic fields at very low temperature [6–9], only very few materials were elusively suggested to fall naturally into the EI ground state so far. The first experimental suggestion was TmSe$_{1-x}$Te$_x$ [10–12] and later La-doped SmS [13], which showed anomalous increases of electric resistivity under high pressure and low temperature. Recently, more detailed discussions were carried out on the temperature-driven transition of 1T-TiSe$_2$ [14–27]. This case, however, has been heavily debated since the insulating property itself

is not observed and the transition apparently involves a charge ordering with a lattice modulation [14–21,23,27]. That is, the EI mechanism has to compete with others such as the Jahn-Teller effect or the charge-density-wave (CDW) formation [17,18]. At the center of this debate is the complexity of the band structure, valence-band holes at the center of the Brillouin zone (BZ) and excited electrons in three conduction bands at the BZ boundary [20], which inevitably involves a nonzero momentum phonon in opening a band gap.

On the other hand, Ta$_2$NiSe$_5$ was very recently proposed as an EI even at room temperature and ambient pressure [28–34]. In contrast to 1T-TiSe$_2$, Ta$_2$NiSe$_5$ has a direct (zero or negative) band gap above the transition temperature $T_c \approx 326$ K [30,31] without any CDW involved. The insulating state at low temperature is evident in a transport measurement [35] and an angle-resolved photoemission spectroscopy (ARPES) work [28,29,32]. Thus, Ta$_2$NiSe$_5$ has obvious merits to clarify the exciton condensation. Ta$_2$NiSe$_5$ is a layered material [35,36] and each layer, as illustrated in Fig. 1, has two Ta and one Ni chains sandwiched by Se atoms within an orthorhombic unit cell [35,36]. It undergoes a second-order phase transition to a monoclinic structure at ∼326 K with an anomaly in electric resistivity [35]. ARPES experiments revealed a part of the band gap below the Fermi level and its enlargement with the unusual flattening of the valence band edge as the temperature decreases [28,29,32]. A model calculation interpreted these observations as the indication of the EI state [32]. A recent optical spectroscopy experiment measured the temperature-dependent optical gap of Ta$_2$NiSe$_5$ [33,34]. Nevertheless, the strong interband interaction, which is the key feature of the EI phase, has not been unveiled yet.

In this work, we investigate the real-space electronic states of the EI phase in Ta$_2$NiSe$_5$. Atom-resolved local density of states in real space was obtained using scanning tunneling microscopy (STM) and spectroscopy (STS), which demonstrates the energy gap with sharp peaks at gap edges, corresponding
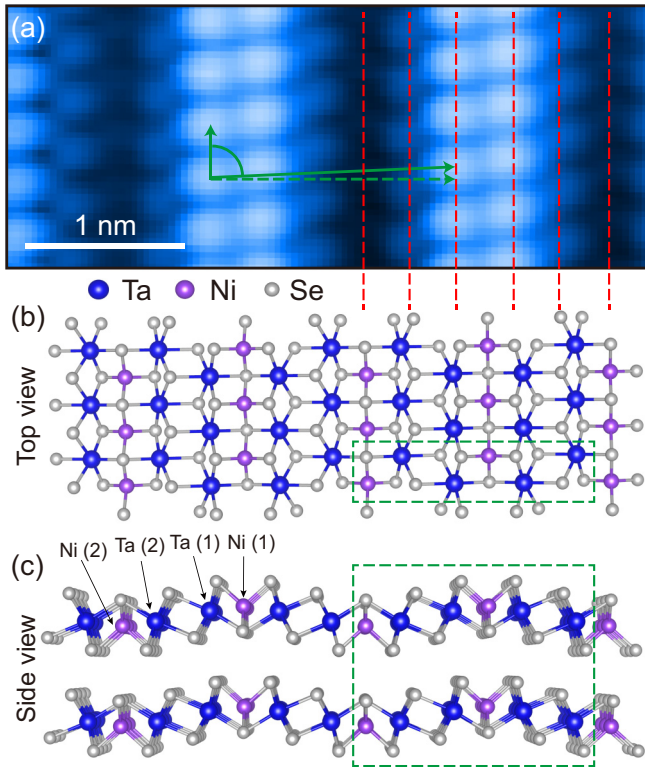
*yeom@postech.ac.kr

FIG. 1. STM topography and structure model. (a) Atom-resolved STM topography at 78 K for Ta_2NiSe_5 (sample bias $V = 250$ mV and the set current 300 pA). The primitive vectors of the monoclinic unit cell are illustrated (green arrows) with deviating slightly from those of the undistorted orthorhombic unit cell (dashed arrow). (b),(c) Structure model of orthorhombic Ta_2NiSe_5 with its unit cell in dashed boxes. Red dashed lines connect the atomic positions of the structure model to those of the STM topography.

to the flat renormalized band dispersion. Moreover, the orbital characters of band edges were inverted in the insulating phase, which is evidence of the strong electron-hole band interaction. The excitonic model calculations revealed that the orbital character inversion also implies the semimetallic band structure in the high-temperature phase. This leads us to conclude that the EI formation is close to the BCS regime rather than the Bose-Einstein condensation within the conventional theory of the EI phase.

Single crystals of Ta_2NiSe_5 were grown using the chemical vapor transport method [37], which were cleaved *in situ* for STM and STS measurements. STM experiments were conducted using commercial cryogenic STMs (Omicron and Unisoku), for 300 and 78 K, respectively. STM topographies were obtained by a constant current mode and a lock-in amplifier was utilized to measure the differential tunneling conductance (dI/dV). The density functional theory (DFT) calculations were performed by using the full-potential linearized augmented plane-wave band method, as implemented in the WIEN2Kpackage [38] with the generalized gradient approximation (GGA) for the exchange correlation [39]. The Brillouin zone integration was done with a $28 \times 28 \times 6$ k mesh and the plane-wave cutoff was $R_{MT}K_{max} = 7$. The Falicov-
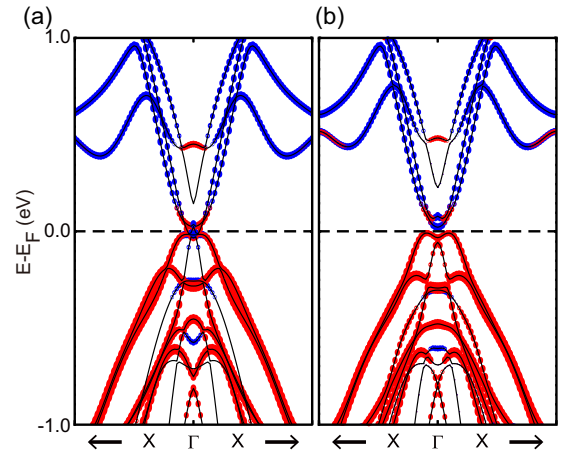

FIG. 2. Structural phase transition and band structures. (a) Calculated band structure of orthorhombic Ta_2NiSe_5 (the high-temperature phase) with experimental lattice parameters. It is composed of Ta $5d$ conduction bands (blue) and Ni $3d$ valence bands (red) with a negative band gap. (b) Similar band structure for monoclinic Ta_2NiSe_5 (the low-temperature phase) without any excitonic interaction.

Kimball model was used for the exciton model calculation [40].

The STM topography taken at 78 K is shown in Fig. 1(a). The topography is largely bias independent within a relevant energy range of ± 1 eV, indicating the lack of significant electronic effects such as charge orders or CDW. This is important for the discussion of the transition mechanism. The bias independence implies that the topography is mainly due to the corrugation of the surface Se layer. Indeed, the topographic contrast matches well with the corrugation of the structure model [Figs. 1(b) and 1(c)] and the x-ray experiment [36]. The lattice constants measured by STM are $a = 3.5$ Å and $c = 15.4$ Å with a monoclinic unit cell in good agreement with the x-ray result for the phase below T_c. Note that this monoclinic structure is a result of the structural transition from an orthorhombic structure at a similar temperature to the electronic transition. Nevertheless, the effect of the structural phase transition on the electronic structure is expected to be negligible compared to the band gap formed through the electronic transition [28,29,32,33]. Our own band-structure calculations for orthorhombic and monoclinic structures (Fig. 2) confirm that the band gap opening due to the structural transition is marginal ($\sim$30 meV) [41]. Moreover, the entropy change associated with the transition was found to originate mainly from the electronic structure [33]. These results make us focus on the electronic transition.

The electronic phase transition is investigated by STS measurements, $[(dI/dV)/(I/V)]$, which reveals the spatial distribution of local density of states (LDOS) with sub-atomic resolution [41,42]. The room-temperature STS data observe finite density of states around the Fermi level although Ta_2NiSe_5 is reported to have T_c of 326 K (Fig. 3). It obviously reflects the gradual nature of the second-order phase transition with the incomplete gap opening at room temperature together with the thermal broadening of spectral features. In stark contrast, the null density of states near the Fermi level is
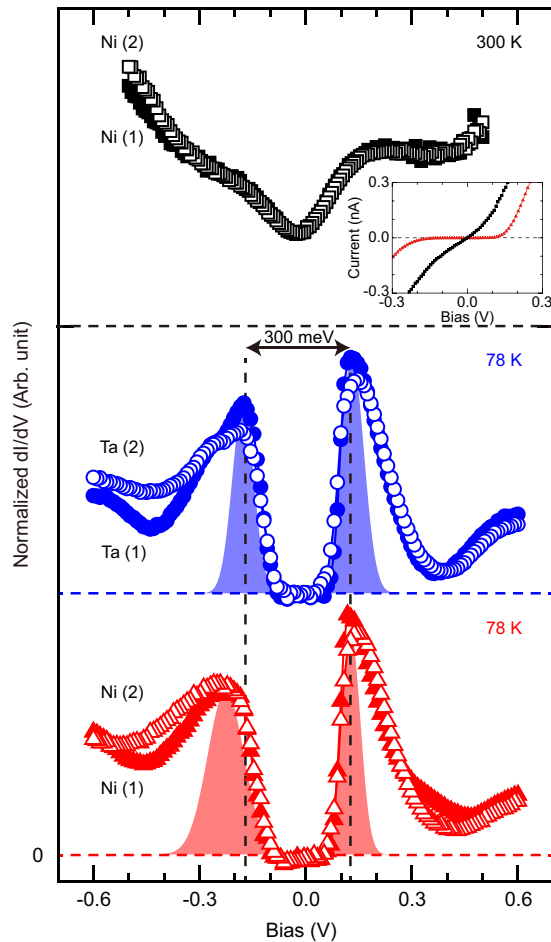
FIG. 3. Tunneling spectroscopic results at 78 and 300 K. Scanning tunneling spectroscopy [$(dI/dV)/(I/V)$] data above different Ni (red triangles) and Ta (blue circles) sites (shown in Fig. 1) at 78 K, which are compared with the corresponding data on Ni sites (black squares) at 300 K. The 300-K data are uniform over different Ni or Ta sites. The inset shows the tunneling current plot (*I-V*) at 78 (red) and 300 K (black). The horizontal dashed lines indicate the null spectral intensity.

clear at 78 K (Fig. 3), which evidences an insulating state at low temperature. The metal-insulator phase transition is well supported by the tunneling conductance itself shown in the inset. The energy gap is as large as 300 meV with distinct spectral peaks at gap edges.

The DFT calculations (Fig. 2) cannot explain this huge energy gap even with the structural distortion, and therefore substantial many-body interactions should be introduced for the electronic phase transition. Before we discuss the interband electron-hole interaction, we consider other types of possible many-body interactions. The on-site Coulomb repulsion (or intraband interaction, U) can be reasonably excluded. We performed a standard GGA $+ U$ calculation for the low-temperature structure to take into account of this effect with a well-referenced value of $U = 5$ eV [43] of Ni $3d$. It turns out that the energy gap is still closed in this calculation [41]. This is because Ta$_2$NiSe$_5$ has a large bandwidth (w), leading to a small value of U/w, the order parameter of a Mott transition. On the other hand, the possibility of the electron-phonon

interaction has to be considered more carefully. Indeed, the electron-phonon interaction is always present and can compete or cooperate with the electron-hole interaction [44]. The previous theoretical study, however, revealed that the electron-phonon interaction cannot open the energy gap solely without the electron-hole interaction but assists the gap opening with a finite electron-hole interaction [31]. Based on this theory, the contribution of the electron-phonon interaction on the energy gap can be quantitatively estimated. Using the DFT calculation [41], we first estimate the phonon momentum q and mode (ν) -dependent electron-phonon coupling constants $\lambda_{q\nu}$ at the Γ point [45]. The largest value of $\lambda_{q\nu}$ at Γ is 0.1256. If we put this value in the above-mentioned theory [31] to fit the observed gap size of the present system, the energy gap enhancement by the electron-phonon coupling is only a few tens of meV [41]. This is not a negligible gap size but is obviously not a major contribution to the transition. Note that the current estimation of the electron-phonon contribution has the uncertainty within the accuracy of the DFT calculation for the high-temperature phase. This gap enhancement is within the energy scale of the relevant phonons [46] and the gap size induced by the structural transition discussed above. Thus, we suggest that the electronic phase transition is driven mainly by the electron-hole interaction while it can still be enhanced by the interaction with phonons. We can thus focus on the EI scenario proposed in this material [28].

The spectral features in Fig. 3 are indeed in good agreement with the EI scenario. Strong peaks at the gap edges would correspond to the flat band edges, which is one of the characteristics of the EI phase [2]. This is also consistent with the flat valence band maximum observed in ARPES measurements [28,29,32]. The asymmetry of the peaks reflects the different band dispersion of those flat band edges in the valence and conduction bands as shown below. These spectral features are commonly shown in both calculations for the density of states with the excitonic model and our STS spectrum with Feenstra normalization method [41]. A detailed discussion on the different spectral shapes is given below with Fig. 4.

Although the optical gap in the low-temperature phase of Ta$_2$NiSe$_5$ was measured in the previous research [33], the single-particle energy spectrum with the energy gap is identified in the present study. The reported optical gap ($\sim$160 meV) [33], which was assigned with nearly zero optical conductivity, seems to correspond to the energy window with zero density of states in our STS measurement. Moreover, a broad peak in optical conductivity at 300–400 meV seems consistent with the present peak-to-peak energy gap [33]. The valence-band maximum relative to the Fermi level was measured as -175 meV in the previous ARPES study [29], which agrees excellently with the filled-state resonance peak in the STS measurement. Thus, the energy gap of the low-temperature phase is consistently quantified.

Beyond the energy gap, the spatial distribution of electronic states is investigated in our STS measurements crossing Ta and Ni chains. The differences in point spectra (Fig. 3) are also demonstrated in a spatially resolved LDOS map at 78 K [Fig. 4(a)]. Distinct features are observed around 125 (◄) and -175 meV (◄), which correspond to aforementioned edges of valence and conduction bands, and these states are
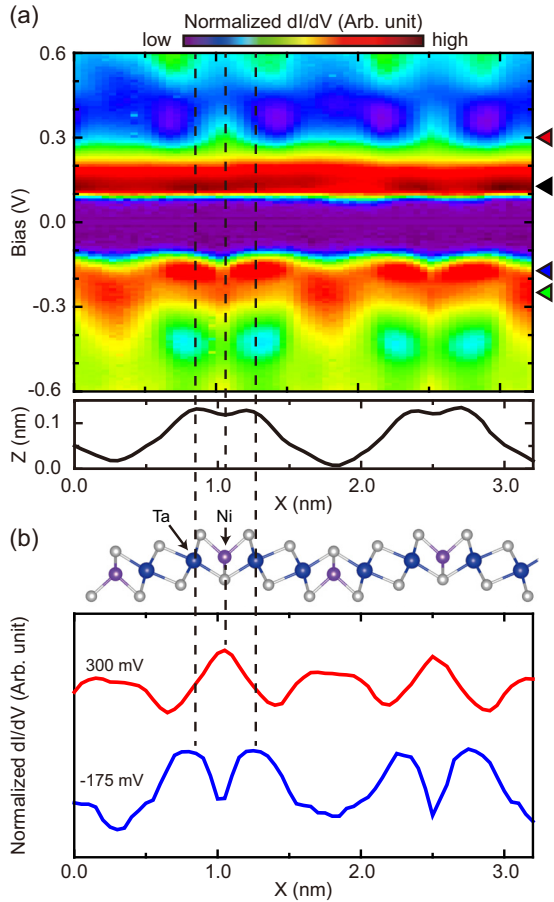
FIG. 4. Spatial distribution of electronic states at 78 K. (a) Normalized dI/dV plot of a line STS measurement at 78 K crossing the Ta and Ni chains (upper) with the topographic profile (lower). (b) Normalized dI/dV profiles with the corresponding structure model at empty (300 mV) and filled (-175 mV) states. The profile at 300 mV is vertically shifted for clarification.

FIG. 5. Two-band exciton model. Band-gap opening and band character inversion at Γ, which are induced by the exciton condensation. (a) Model band structure without the exciton interaction as simplified from the DFT result (Fig. 2). (b) Band structure after including excitonic interaction with an order parameter of $\Delta = 150$ meV. (c),(d) Spectral weights of the valence and conduction bands in the excitonic phase of (b). These weights are also represented by sizes of blue (Ta $5d$) and red (Ni $3d$) dots in (b).

important for the exciton formation. Both of them carry satellite features at 300 (◄) and -250 meV (◄), respectively, which have distinct spatial distributions as shown in the figure. While the feature at 125 meV (◄) has little spatial modulation, that at 300 meV (◄) is well localized on Ni sites. On the other hand, the spectral features at -175 (◄) and -250 meV (◄) are localized at Ta and Ni sites, respectively. Note that this localization of each state corresponds to the difference of the spectral intensity in Fig. 3. This spatial LDOS distribution unveils an important aspect of the gap formation. The DFT calculation for Ta_2NiSe_5 tells us that the bands near the Fermi level are simply composed of parabolic valence and conduction bands from mainly Ni $3d$ and Ta $5d$ orbitals, respectively [30,31]. Our own calculation also confirms this simple band structure (Fig. 2). This contradicts with the STS results where the valence-band maximum is localized strongly on Ta and the conduction-band minimum has a substantial contribution from Ni atoms. Thus, the strong band renormalization has to be involved in the gap-formation transition between Ta and Ni orbitals or conduction- and valence-band edges.
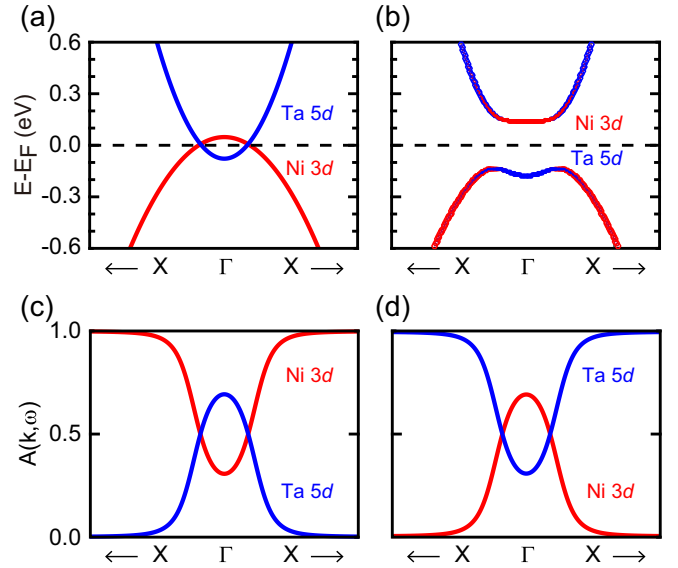
The energy gap formation is further investigated by model calculations [40,41]. As discussed above, the DFT calculation for the noninteracting band structure with the lattice parameters measured by experiments yields a semimetallic phase with a small negative band gap (~ -50 meV) as shown in Fig. 2(a). In the previous calculation, the conduction (valence) bands were shifted upward (downward) by adding (subtracting) an arbitrary orbital-dependent potential to yield a preassumed positive band gap for the high-temperature phase [31]. However, we cannot find any justification for such an artificial gap opening. As the minimal set of a model Hamiltonian, we extract two bands, each from the valence and the conduction band [Fig. 5(a)]. When the coupling of electrons and holes is introduced as a perturbation, the eigenstates near the Fermi level are renormalized with the energy gap opened [Fig. 5(b)]. The gap size depends on the coupling strength (Δ), which is related with the exciton binding energy. The renormalized band dispersion at the gap edges is flat together with the substantial hybridization of Ni $3d$ and Ta $5d$ orbitals. The STS measurements are largely reproduced by this two-band model calculation with an order parameter $\Delta = 150$ meV as shown in Fig. 5(b). That is, the energy gap is opened with a size of 300 meV ($\approx 2\Delta$) and dominant orbital characters at band edges are inverted due to the exciton formation. This inversion is well visualized by the spectral weights of valence [Fig. 5(c)] and conduction bands [Fig. 5(d)] in the EI phase; Ta $5d$ is stronger than Ni $3d$ near the Γ point in the valence band and vice versa in the conduction band. Moreover, we can qualitatively estimate the spatial distribution of the electronic states at the valence band maximum from the model calculation. The stronger spectral weight of Ta $5d$ implies that we have

larger density of states on Ta chains than on Ni chains, which is consistent with the normalized dI/dV profile at the valence band edge (-175 mV) in Fig. 4(b).

The major limitation of the simple model is that the experiment observes a relatively well-delocalized state at the conduction band minimum together with the Ni-localized state. This might be because Ta_2NiSe_5 has two degenerate conduction bands and the interaction between these two and the valence band can be more complex than our model. Nevertheless, the present result indicates unambiguously that the observed localization of the valence-band edge state at Ta chains cannot be explained without the exciton formation. Moreover, this observation is in contradiction with the semiconductor-to-EI scenario proposed earlier [31]. We performed similar model calculations starting from the semiconducting bare band structure and found no inversion of the dominant band characters at edges [41]. In other words, the state at the valence band maximum should have been localized at Ni chains if Ta_2NiSe_5 were a semiconductor in noninteracting phase. That is, the band character inversion is strong evidence of both the exciton formation and the semimetallic (or zero-gap) bare band structure at high temperature. It is largely consistent with optical spectroscopy data indicating a zero-gap semiconductor at high temperature [33].

Another limitation is that our simple model Hamiltonian does not take into account the electron-phonon interaction, which must be entangled with the excitonic interaction. As discussed above, while its contribution to the energy gap is estimated not to be a major one, the electron-phonon interaction assists the excitonic condensation [31,44]. Thus, more accurate quantification of the electron-phonon contribution is necessary. In addition, a recent study reported the exciton-phonon coupling mode in the low-temperature phase [47], which makes the further investigation on phonons interesting.

Summarizing all results, Ta_2NiSe_5 has a metal-insulator transition from a semimetallic noninteracting phase through the strong interband interaction. No other mechanism than EI can solely and plausibly explain these findings together with the experimental data accumulated up to now, such as the band dispersion renormalization. Moreover, the present result indicates that the EI phase in this material is close to the BCS mechanism rather than the Bose-Einstein condensation based on the conventional theory [2,3,5]. Within this mechanism, the phases of excitons are not coherent above T_c but, as the temperature is lowered, excitons become gradually coherent and spontaneously condense, opening the band gap. It is notable that the condensation starts from a higher temperature than room temperature in contrast to BCS superconductors. This is because the binding energy of excitons is two orders of magnitude greater than that of Cooper pairs in BCS superconductors. However, a very recent paper proposed the possibility of a small-gap semiconducting phase above the transition temperature due to preformed excitons in spite of the noninteracting semimetallic bands in Ta_2NiSe_5 [48]. Nevertheless, one of our main observations, the orbital character inversion that is the hallmark of a semimetallic noninteracting band, is consistent with this recent paper. The existence of preformed excitons above the transition temperature has to be addressed in future works. The further control and manipulation of the exciton condensates are highly promising in Ta_2NiSe_5 with its extremely high transition temperature.

[1] M. Imada, A. Fujimori, and Y. Tokura, Rev. Mod. Phys. **70**, 1039 (1998).

[2] D. Jérome, T. M. Rice, and W. Kohn, Phys. Rev. **158**, 462 (1967).

[3] B. I. Halperin and T. M. Rice, Rev. Mod. Phys. **40**, 755 (1968).

[4] N. W. Ashcroft and N. D. Mermin, *Solid State Physics* (Cengage Learning, Boston, 1976), pp. 626–628.

[5] F. X. Bronold and H. Fehske, Phys. Rev. B **74**, 165107 (2006).

[6] R. T. Payne, Phys. Rev. Lett. **21**, 284 (1968).

[7] Y. F. Suprunenko, V. Cheianov, and V. I. Fal'ko, Phys. Rev. B **86**, 155405 (2012).

[8] L. Du, X. Li, W. Lou, G. Sullivan, K. Chang, J. Kono, and R.-R. Du, Nat. Commun. **8**, 1971 (2017).

[9] Z. Zhu, R. D. McDonald, A. Shekhter, B. J. Ramshaw, K. A. Modic, F. F. Balakirev, and N. Harrison, Sci. Rep. **7**, 1733 (2017).

[10] J. Neuenschwander and P. Wachter, Phys. Rev. B **41**, 12693 (1990).

[11] B. Bucher, P. Steiner, and P. Wachter, Phys. Rev. Lett. **67**, 2717 (1991).

[12] P. Wachter, B. Bucher, and J. Malar, Phys. Rev. B **69**, 094502 (2004).

[13] P. Wachter, A. Jung, and P. Steiner, Phys. Rev. B **51**, 5542 (1995).

[14] F. J. Di Salvo, D. E. Moncton, and J. V. Waszczak, Phys. Rev. B **14**, 4321 (1976).

[15] Y. Yoshida and K. Motizuki, J. Phys. Soc. Jpn. **49**, 898 (1980).

[16] Th. Pillo, J. Hayoz, H. Berger, F. Lévy, L. Schlapbach, and P. Aebi, Phys. Rev. B **61**, 16213 (2000).

[17] K. Rossnagel, L. Kipp, and M. Skibowski, Phys. Rev. B **65**, 235101 (2002).

[18] T. E. Kidd, T. Miller, M. Y. Chou, and T.-C. Chiang, Phys. Rev. Lett. **88**, 226402 (2002).

[19] H. Cercellier, C. Monney, F. Clerc, C. Battaglia, L. Despont, M. G. Garnier, H. Beck, P. Aebi, L. Patthey, H. Berger, and L. Forró, Phys. Rev. Lett. **99**, 146403 (2007).

[20] C. Monney, H. Cercellier, F. Clerc, C. Battaglia, E. F. Schwier, C. Didiot, M. G. Garnier, H. Beck, P. Aebi, H. Berger, L. Forró, and L. Patthey, Phys. Rev. B **79**, 045116 (2009).

[21] C. Monney, E. F. Schwier, M. G. Garnier, N. Mariotti, C. Didiot, H. Beck, P. Aebi, H. Cercellier, J. Marcus, C. Battaglia, H. Berger, and A. N. Titov, Phys. Rev. B **81**, 155104 (2010).

[22] J. van Wezel, P. Nahai-Williamson, and S. S. Saxena, Phys. Rev. B **81**, 165109 (2010).

[23] C. Monney, C. Battaglia, H. Cercellier, P. Aebi, and H. Beck, Phys. Rev. Lett. **106**, 106404 (2011).

[24] M. Cazzaniga, H. Cercellier, M. Holzmann, C. Monney, P. Aebi, G. Onida, and V. Olevano, Phys. Rev. B **85**, 195111 (2012).

[25] G. Monney, C. Monney, B. Hildebrand, P. Aebi, and H. Beck, Phys. Rev. Lett. **114**, 086402 (2015).

[26] H. Watanabe, K. Seki, and S. Yunoki, Phys. Rev. B **91**, 205135 (2015).

[27] A. Kogar, M. S. Rak, S. Vig, A. A. Husain, F. Flicker, Y. I. Joe, L. Venema, G. J. MacDougall, T. C. Chiang, E. Fradkin, J. van Wezel, and P. Abbamonte, Science **358**, 1314 (2017).

[28] Y. Wakisaka, T. Sudayama, K. Takubo, T. Mizokawa, M. Arita, H. Namatame, M. Taniguchi, N. Katayama, M. Nohara, and H. Takagi, Phys. Rev. Lett. **103**, 026402 (2009).

[29] Y. Wakisaka, T. Sudayama, K. Takubo, T. Mizokawa, N. L. Saini, M. Arita, H. Namatame, M. Taniguchi, N. Katayama, M. Nohara, and H. Takagi, J. Supercond. Nov. Magn. **25**, 1231 (2012).

[30] T. Kaneko, T. Toriyama, T. Konishi, and Y. Ohta, J. Phys.: Conf. Ser. **400**, 032035 (2012).

[31] T. Kaneko, T. Toriyama, T. Konishi, and Y. Ohta, Phys. Rev. B **87**, 035121 (2013).

[32] K. Seki, Y. Wakisaka, T. Kaneko, T. Toriyama, T. Konishi, T. Sudayama, N. L. Saini, M. Arita, H. Namatame, M. Taniguchi, N. Katayama, M. Nohara, H. Takagi, T. Mizokawa, and Y. Ohta, Phys. Rev. B **90**, 155116 (2014).

[33] Y. F. Lu, H. Kono, T. I. Larkin, A. W. Rost, T. Takayama, A. V. Boris, B. Keimer, and H. Takagi, Nat. Commun. **8**, 14408 (2017).

[34] T. I. Larkin, A. N. Yaresko, D. Pröpper, K. A. Kikoin, Y. F. Lu, T. Takayama, Y.-L. Mathis, A. W. Rost, H. Takagi, B. Keimer, and A. V. Boris, Phys. Rev. B **95**, 195144 (2017).

[35] F. J. Di Salvo, C. H. Chen, R. M. Fleming, J. V. Waszczak, and R. G. Dunn, J. Less Common Met. **116**, 51 (1986).

[36] S. A. Sunshine and J. A. Ibers, Inorg. Chem. **24**, 3611 (1985).

[37] S. Y. Kim, Y. Kim, C.-J. Kang, E.-S. An, H. K. Kim, M. J. Eom, M. Lee, C. Park, T.-H. Kim, H. C. Choi, B. I. Min, and J. S. Kim, ACS Nano **10**, 8888 (2016).

[38] P. Blaha, K. Schwarz, G. Madsen, D. Kvasnicka, and J. Luitz, *WIEN2k* (Karlheinz Schwarz, Techn. Universität Wien, Austria, 2001).

[39] J. P. Perdew, K. Burke, and M. Ernzerhof, Phys. Rev. Lett. **77**, 3865 (1996).

[40] L. M. Falicov and J. C. Kimball, Phys. Rev. Lett. **22**, 997 (1969).

[41] See Supplemental Material at http://link.aps.org/supplemental/10.1103/PhysRevB.99.075408 for the detailed calculations, which includes Refs. [31,36,38–40,42,43,49–58].

[42] R. M. Feenstra, Phys. Rev. B **50**, 4561 (1994).

[43] C. Schuster, M. Gatti, and A. Rubio, Eur. Phys. J. B **85**, 325 (2012).

[44] T. Kaneko, B. Zenker, H. Fehske, and Y. Ohta, Phys. Rev. B **92**, 115106 (2015).

[45] Phonon modes at the Γ point are associated with the structural phase transition between orthorhombic and monoclinic structures.

[46] T. I. Larkin, R. D. Dawson, M. Höppner, T. Takayama, M. Isobe, Y.-L. Mathis, H. Takagi, B. Keimer, and A. V. Boris, Phys. Rev. B **98**, 125113 (2018).

[47] D. Werdehausen, T. Takayama, M. Höppner, G. Albrecht, A. W. Rost, Y. Lu, D. Manske, H. Takagi, and S. Kaiser, Sci. Adv. **4**, eaap8652 (2018).

[48] K. Sugimoto, S. Nishimoto, T. Kaneko, and Y. Ohta, Phys. Rev. Lett. **120**, 247602 (2018).

[49] V. I. Anisimov, I. V. Solovyev, M. A. Korotin, M. T. Czyżky, and G. A. Sawatzky, Phys. Rev. B **48**, 16929 (1993).

[50] V. I. Anisimov, F. Aryasetiawan, and A. I. Lichtenstein, J. Phys.: Condens. Matter **9**, 767 (1997).

[51] K. Lejaeghere *et al.*, Science **351**, 1415 (2016).

[52] G. Prandini, A. Marrazzo, I. E. Castelli, N. Mounet, and N. Marzari, npj Comput. Mater. **4**, 72 (2018).

[53] S. Baroni, S. de Gironcoli, A. Dal Corso, and P. Giannozzi, Rev. Mod. Phys. **73**, 515 (2001).

[54] P. Giannozzi *et al.*, J. Phys.: Condens. Matter **21**, 395502 (2009).

[55] J. A. Stroscio, R. M. Feenstra, and A. P. Fein, Phys. Rev. Lett. **57**, 2579 (1986).

[56] R. M. Feenstra, Phys. Rev. B **44**, 13791 (1991).

[57] A. Villan, Phys. Chem. Chem. Phys. **19**, 27166 (2017).

[58] J. A. Stroscio and W. J. Kaiser (Eds.), *Methods of Experimental Physics*, Vol. 27 (Academic, Boston, 1993), Chap. 4.